Ab initio based tight-binding molecular dynamics simulation of the sticking and scattering of O_2/Pt(111)

A. Groß[a)]
Abteilung Theoretische Chemie, Universität Ulm, D-89069 Ulm, Germany

A. Eichler and J. Hafner
Institut für Materialphysik and Center for Computational Materials Science, Universität Wien, A-1090 Wien, Austria

M. J. Mehl and D. A. Papaconstantopoulos
Naval Research Laboratory, Center for Computational Materials Science, Washington, DC 20375-5345

(Received 10 January 2006; accepted 9 March 2006; published online 5 May 2006)

The sticking and scattering of O_2/Pt(111) has been studied by tight-binding molecular dynamics simulations based on an *ab initio* potential energy surface. We focus, in particular, on the sticking probability as a function of the angle of incidence and the energy and angular distributions in scattering. Our simulations provide an explanation for the seemingly paradox experimental findings that adsorption experiments suggest that the O_2/Pt(111) interaction potential should be strongly corrugated while scattering experiments indicate a rather small corrugation. The potential energy surface is indeed strongly corrugated which leads to a pronounced dependence of the sticking probability on the angle of incidence. The scattered O_2 molecules, however, experience a rather flat surface due to the fact that they are predominantly scattered at the repulsive tail of the potential.
 [DOI: 10.1063/1.2192512]

I. INTRODUCTION

The adsorption dynamics of molecules is not only of fundamental interest but also of technological relevance since adsorption corresponds to the first step in any catalytic reaction at surfaces. In particular, the interaction of hydrogen with metal surfaces has been studied intensively, both experimentally[1–3] as well as theoretically.[4–18] Although there is some surface temperature dependence in the H_2/metal dynamics, in particular, in hydrogen thermal desorption[19] and scattering from metal surfaces,[20,21] the influence of the surface motion on the *adsorption* probabilities is usually minor because of the large mass mismatch between hydrogen and the metal substrate atoms. Hence, in the theoretical simulation of the H_2 adsorption dynamics the influence of the surface recoil can usually be neglected, and the adsorption process can be safely described taking only the six H_2 degrees of freedom into account. It is now standard[22] that the potential energy surfaces (PESs) used in these dynamical simulations are derived from first-principles calculations mainly based on density functional theory (DFT).

In the case of the O_2 adsorption on Pt(111), the mass mismatch with the substrate atoms is not as favorable as for hydrogen. Furthermore, O_2 can adsorb both molecularly as well as dissociatively.[23–29] This means that in the adsorption dynamics the influence of the substrate degrees of freedom can no longer be neglected since molecular adsorption can only occur via energy transfer to the substrate.[30] This makes any *ab initio* based dynamical simulation of the O_2 adsorption dynamics much more demanding. As a consequence, there are hardly any realistic simulations addressing the complex scattering and adsorption of O_2/Pt(111), although it has been studied in detail experimentally.[31–37] This interest in the O_2/Pt(111) system has been fueled by the fact that the adsorption of O_2 on Pt is a crucial microscopic reaction step occurring in the car-exhaust catalyst.

Oxygen can adsorb in three different molecular adsorption states on Pt(111).[29] At surface temperatures below 30 K, a weakly bound physisorbed species is stable.[25,26] Chemisorbed peroxolike (O_2^{-2}) and superoxolike (O_2^{-}) molecular states are found up to surface temperatures of about 100 K.[24,27] The assignment of the chemisorbed molecular states has been confirmed by total-energy calculations[38,39] using DFT within the generalized gradient approximation[40] (GGA) for the exchange-correlation effects.

Molecular beam experiments addressing the adsorption of O_2 on Pt(111) have found that the sticking probability first exhibits a strong decrease as a function of the kinetic energy,[32] and then after passing a minimum at approximately 0.15 eV the sticking probability levels off at a value of about 0.3.[32,37] We have recently performed *ab initio* based tight-binding molecular dynamics simulation of the sticking of O_2/Pt(111).[41] We have demonstrated that in this system the whole adsorption probability as a function of the kinetic energy can be understood in terms of trapping into chemisorbed molecular precursor states. Furthermore, by simple steric arguments we were able to explain the experimental observation[33,36,37] that O_2 does not dissociate on cold Pt(111) surfaces even at kinetic energies that are much greater than the dissociation barrier.

In this paper, we extend this study by particularly focusing on the sticking probability as a function of the angle of

[a)]Electronic mail: axel.gross@uni-ulm.de

incidence and the energy and angular distributions in scattering. Our results are in good agreement with existing experimental data. In particular, we reproduce the seemingly paradox experimental findings that scattered O_2 molecules experience a rather flat Pt(111) surface[34] while the adsorption results suggest that the interaction potential should strongly vary as a function of the lateral coordinates.[32] The potential energy surface is indeed strongly corrugated which is reflected in the pronounced dependence of the sticking probability on the angle of incidence which does *not* follow normal energy scaling. Still the scattered molecules show a near-specular distribution indicative of a flat surface. This is caused by the fact that most molecules are directly scattered at the repulsive tail of the potential which exhibits a smaller corrugation.

II. THEORETICAL METHODS

The realistic simulation of the adsorption and scattering of O_2/Pt(111) requires the reliable description of the molecule-surface interaction including the energy transfer to the substrate. Detailed DFT calculations of the O_2/Pt(111) potential energy surface have been performed using the Vienna *ab initio* simulation package[42,43] VASP working in a plane-wave basis. Exchange-correlation effects are described within the gradient-corrected PW91 functional.[40] Details of the computational setup are described in Refs. 38 and 39. The *ab initio* calculated PES has been used to adjust the parameters of the Naval Research Laboratory (NRL) tight-binding (TB) Hamiltonian.[44–46] This approach combines a quantum mechanical description of the molecule-surface interaction with the numerical efficiency of tight-binding calculations which are about three orders of magnitude faster than DFT calculations.

The NRL-TB scheme, unlike other tight-binding methods,[47] does not contain a pair-potential term. Instead, its formulation is based on shifting the *ab initio* eigenenergies ϵ_i by a constant to satisfy the condition

$$E_{\mathrm{tot}} = \sum_{\mathrm{occ}} \epsilon_i, \tag{1}$$

where E_{tot} is the *ab initio* total energy. Both E_{tot} and ϵ_i are matched by a least-squared procedure to the eigenvalues ϵ_i' and the total energy E_{tot}' resulting from solving the generalized Schrödinger equation

$$(\hat{\mathbf{H}} - \epsilon_i' \hat{\mathbf{S}})\psi_i = 0, \tag{2}$$

where $\hat{\mathbf{H}}$ and $\hat{\mathbf{S}}$ are the Hamiltonian and overlap matrices, respectively, in an atomic basis representation $\{\phi_\alpha\}$. The resulting matrix elements contain Slater-Koster parameters which depend on the distance r between two atoms and are parametrized according to

$$P_i = \left(\sum_{k=0}^{4} a_k^{(i)} r^k \right) \exp(-\gamma_i^2 r) f_i(r), \tag{3}$$

where

$$f_i(r) = \frac{1}{1 + \exp[(r - r_i^0)/l]} \tag{4}$$

is a cutoff function. The index i is a multicomponent index that labels the interacting orbitals. The method also contains environment-dependent on-site terms that account for the effects of the local neighborhood on each atom.[44] For further details, we refer to previous calculations.[44–46]

The parameters of the NRL-TB scheme have been adjusted in order to reproduce the results of DFT calculations. As far as the description of the Pt atoms is concerned, the TB parameters were fitted to bulk calculations which have been shown to give a good representation of the pure Pt surface as well.[44] The Pt–O and the O–O TB parameters have been fitted to reproduce the DFT calculations of the O_2/Pt(111) potential energy surface[38,39] with a root mean square error of below 0.1 eV,[41,45] which is in the range of the error of the GGA-DFT calculations. However, while the polynomial appearing in the functional form of the Pt–Pt parameters in Eq. (3) is only expanded up to the first order term, i.e., $k_{\mathrm{max}}^{\mathrm{Pt-Pt}} = 1$, we realized that for the O–O and O–Pt parameters this expansion is not flexible enough to accurately reproduce the O_2/Pt(111) *ab initio* PES. This is due to the fact that in order to describe the processes of bond breaking and bond making at surfaces the Slater-Koster parameters have to be appropriately determined for a wide range of distances. For that reason we expand the polynomial in Eq. (3) for the O–O and O–Pt parameters up to fourth order. This results in an accurate representation of the *ab initio* PES in the whole relevant energy regime, as can also be seen by comparing the fitted PES plotted in Ref. 41 with the *ab initio* PES shown in Ref. 39. It is important to note that in the DFT calculations the PES has only been calculated for fixed positions of the Pt substrate atoms. Thus the coupling of the O_2 molecule to the Pt lattice vibrations has only been modeled on a tight-binding level, not on an *ab initio* level.

Using this *ab initio* based TB Hamiltonian, tight-binding molecular dynamics (TBMD) simulations[48] of the adsorption and scattering of O_2/Pt(111) have been performed. The surface has been modeled in the supercell approach by a slab of five layer thickness. For the fit, the same $c(4\times2)$ surface unit cell as used in the DFT calculations has been employed. The MD simulations have been performed with a time step of 1 fs. The bottom layer of the Pt slab was kept frozen in the MD simulations while all other Pt atoms were treated dynamically, thus allowing energy transfer from the impinging molecule to the substrate. The spin state of the oxygen molecule has not been explicitly considered in the TB simulations. This corresponds to the assumption that the electron spins follow the motion of the nuclei adiabatically and remain in their ground state.

Molecular dynamics simulations have been performed as a function of the incident kinetic energy for different angles of incidence. For each of these initial conditions, between 150 and 300 trajectories have been determined by averaging over random initial lateral positions and orientations. Thus the calculated trapping probabilities have a statistical error of less than $\sqrt{s(1-s)}/\sqrt{150} \approx 0.04$, where s is the trapping probability. A trajectory was considered to correspond to a trap-

ping event when the molecule stayed for more than 2 ps at the surface or if it had transferred more than its initial energy to the surface if the surface temperature was $T_s=0$ K.

No zero-point vibrations were taken into account in the initial conditions. This has been shown to be appropriate for the classical simulation of nonactivated adsorption processes when the decrease in the molecular vibrational zero-point energy is compensated for by the building up of zero-point energies in the other molecular degrees of freedom.[49,50]

For lower kinetic energies, a $c(4\times2)$ surface unit cell has been used while for kinetic energies of 0.6 and 1.1 eV a $c(4\times4)$ surface unit cell has been employed to minimize the interaction between the cells. The simulations were performed within the microcanonical ensemble. In order to model a Pt substrate with a finite surface temperature of 300 K, the pure Pt slab has been equilibrated at the given surface temperature for at least 1 ps. Three different slab configurations of the microcanonical ensemble have then been used randomly as the initial conditions for the thermalized substrate in the TBMD simulations. The energy transfer from the O_2 molecule to the substrate does of course lead to a heating up of the substrate because of the finite size of the surface unit cell. However, for higher initial kinetic energies the trapping probability is almost independent of the surface temperature while at lower kinetic energies the heating up only occurs once the molecule has lost so much energy that it cannot leave the surface again. We also coupled the bottom layer of the slab to a heat bath via the generalized Langevin equation which, however, did not change the outcome of the molecular trajectories.

III. RESULTS AND DISCUSSION

In this study, we focus on the trapping and scattering of O_2/Pt(111) as a function of the angle of incidence, while our previous study[41] was mainly concerned with the adsorption probability as a function of the kinetic energy for normal incidence. In order to assess the effect of additional parallel momentum, the results of the TBMD simulations for normal[41] and non-normal incidences are shown together with experimental molecular beam data[32,37] in Fig. 1. Although the theoretical results are systematically larger than the experimental ones, the qualitative trend is well reproduced. An analysis of the simulations revealed that contrary to common belief[33,37] the whole adsorption probability of O_2/Pt(111) as a function of the kinetic energy can be understood in terms of trapping into chemisorbed molecular precursor states. Because of steric hindrance, the impinging O_2 molecules do not directly dissociate, even for kinetic energies higher than the dissociation barrier. The high trapping probability at low kinetic energies is caused by the steering effect[9,50] which becomes quickly suppressed for higher kinetic energies. The leveling off of the trapping probability at higher kinetic energies is caused by dynamic trapping[49,51,52] due to the conversion of the initial kinetic energy into internal molecular degrees of freedom which for this particular system is almost independent from the kinetic energy.

We have now additionally performed TBMD simulations for different incident angles at two kinetic energies, 0.3 and 1.1 eV. In order to allow a realistic comparison with the scattering experiments,[34] in the simulations the Pt(111) substrate has been prepared with a surface temperature of 300 K, and the O_2 molecules had an initial rotational energy of 0.1 eV, typical for molecular beam experiments.[53] The corresponding trapping probability has also been included in Fig. 1 as a function of the normal component of the kinetic energy $E_{\mathrm{kin}}\cos^2\theta_i$. It is obvious that the trapping of O_2/Pt(111) does not obey normal energy scaling, i.e., it is not a function of the normal kinetic energy alone, since the results for non-normal incidence are smaller than those for normal incidence. This already indicates that the corrugation of the potential energy surface plays an important role in the adsorption dynamics.

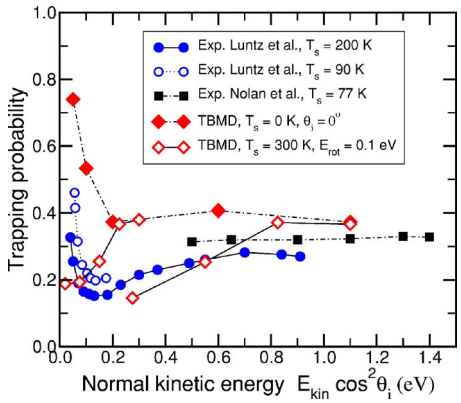

FIG. 1. Trapping probability of O_2/Pt(111) as a function of the kinetic energy for normal incidence. Results of molecular beam experiments for surface temperatures of 90 and 200 K [Luntz *et al.* (Ref. 32)] and 77 K [Nolan *et al.* (Ref. 37)] are compared with tight-binding molecular dynamics simulations for the surface initially at rest ($T_s=0$ K). In addition, the results of TBMD simulations for a surface temperature of $T_s=300$ K, an initial rotational energy of 0.1 eV, total kinetic energies of 0.3 and 1.1 eV, and varying incident angle are plotted as a function of the normal component of the kinetic energy $E_{\mathrm{kin}}\cos^2\theta_i$.

The angular dependence of the trapping probability as a function of the angle of incidence for $E_{\mathrm{kin}}=0.3$ and 1.1 eV is plotted in detail in Fig. 2. The comparison with the experimental results[32] first of all indicates again the systematic overestimation of the trapping probability in the calculations. In order to compare the relative trend as a function of the angle of incidence, we have multiplied the experimental adsorption probability for $E_{\mathrm{kin}}=0.3$ eV in Fig. 2(a) by a factor of 3. The TBMD results show a weaker dependence on the angle of incidence than the molecular beam data, but the suppression of the trapping probability by additional parallel momentum is well reproduced.

As far as the quantitative differences between theory and experiment are concerned, we note that the PW91-GGA functional[40] used in the DFT calculations overestimates the binding energies of the molecular adsorption state by 0.2 eV[38,39,54] compared with the experiment.[23,24] Hence the calculated PES is too attractive, which partially explains the fact that the theoretical sticking probabilities are systematically larger than the experimental ones. However, we would also like to point out that the experimental determination of sticking probabilities for a reactive system represents a challenging task. This is, for example, reflected in Ref. 32 where

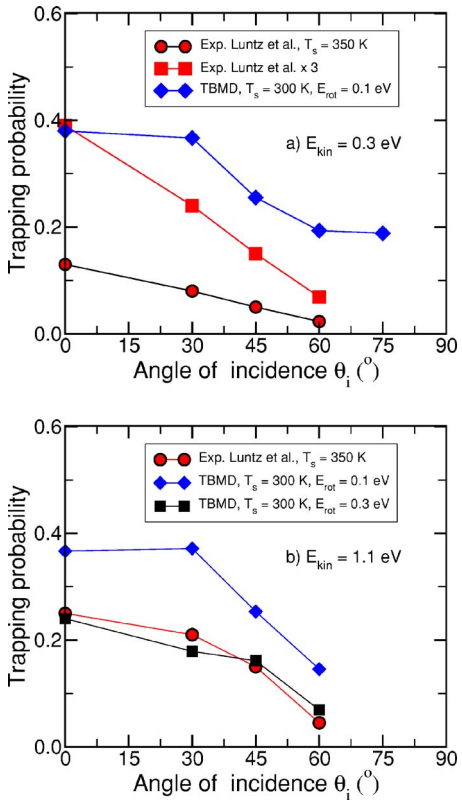

FIG. 2. Trapping probability of O_2/Pt(111) as a function of the angle of incidence for kinetic energies of (a) 0.3 eV and (b) 1.1 eV. Results of molecular beam experiments for surface temperatures of 350 K [Luntz *et al.* (Ref. 32)] are compared with tight-binding molecular dynamics simulations for a surface temperature of 300 K. In (a), the experimental results are additionally scaled with a factor of 3 in order to allow a better comparison with the calculations. The initial rotational energy in the calculations is specified in the legends.

some plotted data for the adsorption probability of O_2/Pt(111) originating from two different experimental runs deviate by up to about 50% for otherwise identical conditions (compare, e.g., Figs. 6 and 8 in Ref. 32). Thus the semiquantitative agreement with experiment and theory is satisfactory, given the uncertainties both in theory as well as experiment, but most important is the fact that the qualitative trends found in the experiment are *all* reproduced by our calculations.

For the kinetic energy of E_{kin}=1.1 eV we have also performed TBMD simulations with an initial rotational energy of 0.3 eV [see Fig. 2(b)]. These results are in excellent agreement with experiment. However, such a high initial rotational energy in the molecular beams seems to be unrealistic,[53] in particular, considering the fact that these high kinetic energies in the molecular beam experiments have been obtained by seeding techniques which usually do not increase the rotational energy of the beams. Still these high-energy results show that experiment and TBMD simulations find very similar relative trends of the trapping as a function of the angle of incidence. The results show, in particular, that the trapping of O_2/Pt(111) is not a function of the total-energy, i.e., the trapping probability also does not obey total energy scaling as has sometimes been assumed to be valid for molecular trapping.

Theoretically, the dependence of the adsorption probability on the angle of incidence has been extensively studied for the dissociation of H_2 on metal surfaces.[17,50,55,56] In these simulations, the substrate had been kept fixed because of the large mass mismatch between hydrogen and the metal atoms. Hence no energy transfer to the substrate and no recoil effects had been taken into account. It is important to note that the trapping of O_2/Pt(111) is dominated by steering effects and dynamic trapping[41] which depend on the corrugation and anisotropy of the potential energy surface and not so much on the energy transfer to the substrate. Hence the previous H_2 studies are also relevant for the system O_2/Pt(111).

Additional parallel momentum leads to a strong suppression of the trapping probability, as Fig. 1 demonstrates. Because of the additional parallel momentum, the incoming molecules traverse the surface unit cell, thereby probing the lateral corrugation of the potential. Therefore the chance that the molecules encounter a high barrier where they are scattered back into the gas phase is increased. Or put differently, the more attractive parts of the potential are not directly accessible due to shadowing effects of the repulsive parts. Thus the variation of the barrier heights, the so-called energetic corrugation,[55] causes the suppression of the sticking, similar to the case of H_2 adsorption.[17,50,55,56]

For an incident angle of 30°, however, the TBMD results show only a very small reduction of the trapping probability; for E_{kin}=1.1 eV and E_{rot}=0.1 eV, there is even a small enhancement compared with the value for normal incidence. This can be explained by the fact that because of the variation of the barrier position there is a larger area in the surface unit cell for non-normal incidence where the beam hits the barrier almost aligned to the local potential gradient.[55,56] At these sites, the total incident energy can be more effective in overcoming local barriers. This geometric corrugation, i.e., the variation of the distance of the barriers from the surface,[55] can thus enhance the sticking probability for non-normal incidence. However, Fig. 2(b) shows that the dependence of the trapping probability on the angle of incidence also depends on the initial rotational energy. This indicates that there is a considerable coupling between rotations and parallel motion which has also been found in H_2 scattering.[57]

As far as the scattered molecules are concerned, their angular distribution is shown in Fig. 3 for an angle of incidence of 45° and initial kinetic energies of 0.3 and 1.1 eV. The distributions show that there is predominantly in-plane scattering, i.e., the molecules do not significantly change their azimuthal angle. This already suggests that the potential the molecules experience is rather flat. At the higher kinetic energy of 1.1 eV, the azimuthal distribution is somewhat broader and the in-plane scattering is shifted to supraspecular angles, but the scattering distribution is still dominated by in-plane scattering close to the specular direction.

Experimentally, usually only the scattering distribution for in-plane scattering is measured. In Fig. 4, we compare our results for the angular distribution with the experimental data for an initial kinetic energy of 0.46 eV.[34] For the calculated distribution, a polar angular resolution of ±2.5° has been assumed, i.e., for each polar angle θ the scattering events in the intervals $(\theta-2.5°, \theta+2.5°)$ have been summed

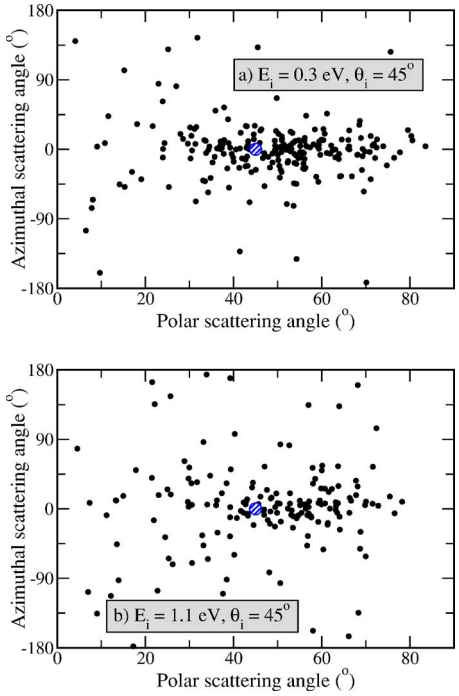

FIG. 3. Calculated angular distribution of O_2 molecules scattered from Pt(111) (surface temperature T_s=300 K) with an angle of incidence of 45° and initial kinetic energies of (a) 0.3 eV and (b) 1.1 eV. The specular direction is indicated by the hatched circle.

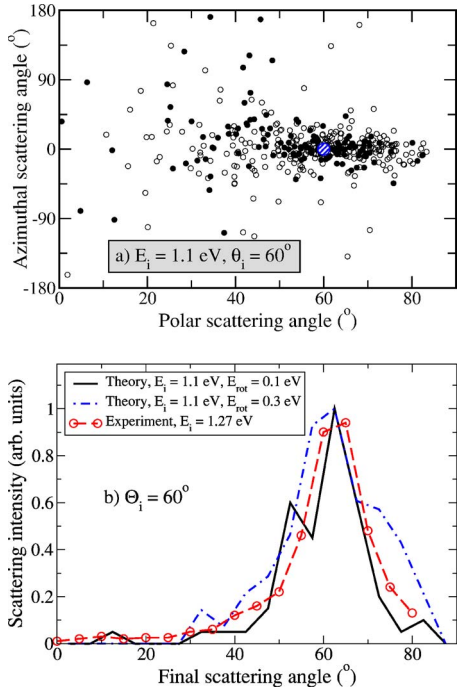

FIG. 5. Angular distribution of O_2 scattered from Pt(111) with an angle of incidence of 60°. (a) Calculated angular distribution (surface temperature T_s=300 K) for initial rotational energies of 0.1 eV (filled circles) and 0.3 eV (open circles). (b) Comparison of the measured and the calculated angular distribution in in-plane scattering for an angle of incidence of 60°. The initial kinetic energy in the experiment was 1.27 eV (Ref. 34) while the TBMD simulations have been performed for an initial energy of 1.1 eV. Theoretical results are shown for both initial rotational energies of 0.1 and 0.3 eV.

up. Furthermore, all scattering events are included where the change of the azimuthal angle has been below ±10°. Still the statistics are relatively poor since in total less than 100 in-plane scattering events per kinetic energy were obtained. This is reflected in the oscillatory structure of the TBMD results. In general, however, the position and width of the experimental distribution are satisfactorily reproduced by the calculations for E_{kin}=0.3 eV. For the higher kinetic energy of 1.1 eV, the distribution is shifted to supraspecular angles, as mentioned above; the width of the distribution, however, is even smaller. In fact, the angular distribution of Ar atoms scattered from Pt(111) is very similar to that of O_2 scattered at the same surface.[34,58] The interaction potential of noble gas atoms with low-index metal surfaces is usually relatively structureless and only weakly corrugated. The similarity between Ar/Pt(111) and O_2/Pt(111) scatterings indicates that also the O_2 scattering corresponds to the reflection from a rather flat surface. The width of the in-plane distribution can be explained by the energy transfer to a vibrating flat surface[34] which leads to a certain width in the distribution of the normal component of the kinetic energy. Together with the conservation of the parallel momentum of the scattered particles this causes the broadened angular distribution around the specular direction in the scattering.

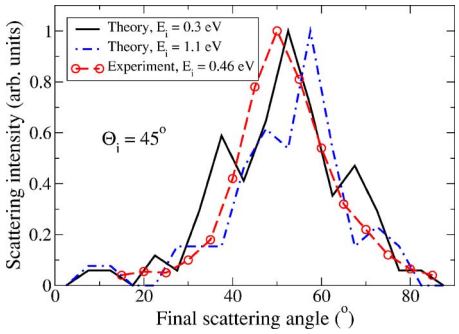

FIG. 4. Comparison of the measured and the calculated angular distribution in in-plane scattering for an angle of incidence of 45°. The initial kinetic energy in the experiment was 0.46 eV (Ref. 34) while the TBMD simulations have been performed for initial energies of 0.3 and 1.1 eV, respectively. For details of the determination of the theoretical distribution, see the text.

However, as already mentioned, the comparison between Figs. 3(a) and 3(b) indicates that at higher kinetic energies the effective corrugation probed by the scattered molecules is somewhat stronger. The results for an angle of incidence of 60° are shown in Fig. 5. It is true that the total scattering distribution shown in Fig. 5(a) for molecules with initial rotational energies of 0.1 and 0.3 eV is still centered around the specular direction in agreement with the experiment. Also the widths of the experimental and the calculated angular distribution are very similar. However, in agreement with experiment[34] we find that the total kinetic energy of the scattered molecules increases up to final polar angles of about 70°, while at an initial kinetic energy of 0.3 eV the final kinetic energy is only weakly dependent on the scattering angle. For scattering at a flat surface one would expect that the total kinetic energy decreases with scattering angle since the component along the surface normal has to be reduced for increasing scattering angle if the parallel component is conserved.

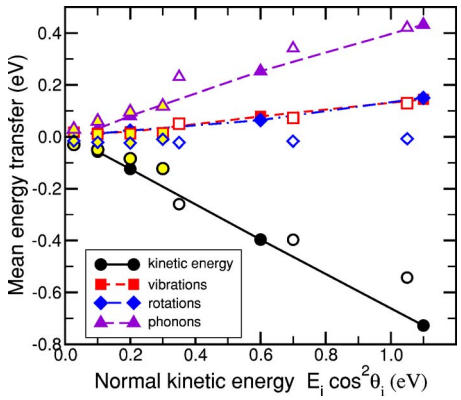

FIG. 6. Calculated mean energy transfer in the scattering of O_2/Pt(111) as a function of the initial normal kinetic energy. The dark filled symbols are for normal incidence for initially nonrotating molecules and the surface atoms at rest, i.e., at a surface temperature of 0 K. The open symbols are obtained in TBMD simulations for varying incident angle, an initial rotational energy of 0.1 eV, and a surface temperature of T_s=300 K.

An important issue in the molecule-surface scattering is the final energy distribution among the different degrees of freedom of the scattered molecules. This distribution is directly linked to the corrugation and anisotropy of the potential energy surface. Unfortunately, in contrast to H_2, for O_2 no state-selective identification of the internal molecular energy distribution is possible experimentally. Hence, the theoretical determination of this distribution is even more important. In Fig. 6, the calculated mean energy transfer into the different molecular and substrate degrees of freedom in the scattering of O_2 from Pt(111) is plotted as a function of the initial normal kinetic energy.

The dark filled symbols denote the values for initially nonrotating O_2 molecules for normal incidence at a Pt(111) surface at rest, i.e., for a surface temperature of T_s=0 K. The values for the different degrees of freedom show a clear linear relationship with respect to the initial kinetic energy. In the scattering event, the molecules lose on the average more than 60% of their initial kinetic energy. Most of this energy, about two-thirds, is transferred to the substrate phonons. The rest is distributed equally among the molecular rotations and vibrations. This energy transfer to the rotations and vibrations amounts to about 10% of the initial kinetic energy for each. This means that there is relatively little vibrational and rotational excitations in the scattering of O_2 from Pt(111).

In Fig. 6, the calculated mean energy transfer is also included for O_2 molecules under non-normal incidence plotted as a function of the normal component of the kinetic energy (open symbols). However, these data correspond to the calculations also presented in Fig. 2, i.e., they have been obtained for an initial rotational energy of 0.1 eV and a surface temperature of T_s=300 K. Thus the effect of the additional rotational motion and the finite surface temperature has to be considered in the comparison with the normal incidence data. Still it is apparent that the non-normal incidence data obey almost the same linear relationship with the normal kinetic energy as the normal incidence data. This is a further indication that the scattered O_2 molecules are directly reflected from a rather flat surface.

The only difference in the energy transfer between the molecules for normal and non-normal incidences can be found for the rotations. This is no surprise, though. For normal incidence, the mean energy transfer to the rotations is relatively small, less than 150 meV even for an initial kinetic energy of 1.1 eV. The molecules under non-normal incidence already have an initial rotational energy of 100 meV, which means that they can both gain and lose rotational energy. The results show that for molecules that are already rotating the scattering is rotationally elastic on the average.

The analysis of the angular and energy distributions of the scattered O_2 molecules suggests that these molecules are indeed scattered from a rather flat surface. This is surprising considering the large corrugation of the O_2/Pt(111) potential energy surface[38,39,41] and the strong deviation of the trapping probability from normal energy scaling (see Figs. 1 and 2). This seeming contradiction can be understood if one takes into account that the scattered molecules are directly reflected from the repulsive part of the potential energy surface, as the analysis of the trajectories confirms. The vast majority of the reflected molecules do not enter the attractive channels of the potential energy surface leading towards the molecular chemisorption sites, i.e., they are not temporarily trapped. Instead, they are reflected from the repulsive tails of the potential energy surface relatively far away from the surface where the PES is much less corrugated and anisotropic. This is particularly true for molecules under non-normal incidence for which the attractive parts of the potential are not directly accessible due to shadowing effects. It is interesting to note that the trapping probability is suppressed by additional rotational motion [see Fig. 2(b)] while the scattering distribution is almost independent of the initial rotational motion of the O_2 molecules [see Fig. 5(b)]. This confirms that the trapping and the scattering dynamics are determined by different parts of the potential energy surface.

The fact that the total kinetic energy of the scattered molecules does not monotonically decrease with increasing scattering angles is an indication that there is still a certain influence of the corrugation on the details of the scattering events. In particular, at high incident kinetic energies the energy distribution of the scattered particles deviates from the behavior expected for scattering from a flat surface. This is caused by the fact that the particles with higher kinetic energies come closer to the surface and that they are reflected from the higher energy regions of the repulsive part of the potential energy surface which is much more strongly corrugated than the low-energy part.

As far as the energy transfer in scattering is concerned, most of the energy is transferred to the substrate phonons. Still it is on the average only less than 40% of the initial kinetic energy. Note that molecular trapping requires that more than the initial kinetic energy is transferred to the substrate; otherwise the particle is eventually scattered back into the gas phase. In spite of the relatively small energy transfer to the substrate phonons, a considerable fraction of the impinging O_2 molecules still becomes molecularly trapped at high kinetic energies (see Fig. 1).

Thus the excitation of substrate phonons upon the impact of the impinging molecules is not sufficient to explain the almost energy-independent trapping probability for higher

kinetic energies. Indeed, an analysis of the trajectories of particles that become trapped indicates that the trapping involves a dynamical precursor,[41] i.e., after impinging these molecules temporarily transfer a large amount of kinetic energy into the internal molecular degrees of freedom of rotations and vibrations and also lateral motion along this surface. This energy is then not available for an escape back into the gas phase. While being dynamically trapped, the particles move back and forth with respect to the surface, thereby transferring more and more energy to the substrate until the particles equilibrate with the surface. This mechanism leads to the relatively large and energy-independent trapping probability at higher kinetic energies.

IV. CONCLUSIONS

By performing *ab initio* based tight-binding molecular dynamics simulations we have addressed the trapping and scattering of O_2/Pt(111). The potential energy surface is strongly corrugated, leading to a significant suppression of the trapping probability for additional parallel momentum. Still the angular distribution and the energy transfer in the scattering of O_2 from Pt(111) are indicative of the reflection from a rather flat surface. The scattering from an apparently flat and inert surface is also reflected in the small vibrational and rotational excitations of the molecules. This seeming contradiction is caused by the fact that the scattered molecules are reflected directly from the repulsive tails of the potential which is less strongly corrugated, while in the trapping the corrugation and anisotropy of the potential energy surface closer to the surface play an important role.

ACKNOWLEDGMENTS

The simulations have been made possible by a grant of computer time at the John-von-Neumann Center for Scientific Computing (NIC) in Jülich, Germany.

[1] K. D. Rendulic and A. Winkler, Surf. Sci. **299/300**, 261 (1994).
[2] C. T. Rettner, H. A. Michelsen, and D. J. Auerbach, J. Chem. Phys. **102**, 4625 (1995).
[3] M. Gostein and G. O. Sitz, J. Chem. Phys. **106**, 7378 (1997).
[4] G. R. Darling and S. Holloway, Rep. Prog. Phys. **58**, 1595 (1995).
[5] A. Groß, Surf. Sci. Rep. **32**, 291 (1998).
[6] G.-J. Kroes, Prog. Surf. Sci. **60**, 1 (1999).
[7] G.-J. Kroes, A. Groß, E. J. Baerends, M. Scheffler, and D. A. McCormack, Acc. Chem. Res. **35**, 193 (2002).
[8] A. Groß, B. Hammer, M. Scheffler, and W. Brenig, Phys. Rev. Lett. **73**, 3121 (1994).
[9] A. Groß, S. Wilke, and M. Scheffler, Phys. Rev. Lett. **75**, 2718 (1995).
[10] G.-J. Kroes, E. J. Baerends, and R. C. Mowrey, Phys. Rev. Lett. **78**, 3583 (1997).
[11] A. Eichler, J. Hafner, A. Groß, and M. Scheffler, Phys. Rev. B **59**, 13297 (1999).
[12] A. Eichler, J. Hafner, A. Groß, and M. Scheffler, Chem. Phys. Lett. **311**, 1 (1999).
[13] H. F. Busnengo, E. Pijper, M. F. Somers, G. J. Kroes, A. Salin, R. A. Olsen, D. Lemoine, and W. Dong, Chem. Phys. Lett. **356**, 515 (2002).
[14] M. F. Somers, D. A. McCormack, G.-J. Kroes, R. A. Olsen, E. J. Baerends, and R. C. Mowrey, J. Chem. Phys. **117**, 6673 (2002).
[15] H. F. Busnengo, E. Pijper, G.-J. Kroes, and A. Salin, J. Chem. Phys. **119**, 12553 (2003).
[16] M. A. Di Cesare, H. F. Busnengo, W. Dong, and A. Salin, J. Chem. Phys. **118**, 11226 (2003).
[17] A. Dianat and A. Groß, J. Chem. Phys. **120**, 5339 (2004).
[18] A. Dianat, S. Sakong, and A. Groß, Eur. Phys. J. B **45**, 425 (2005).
[19] M. J. Murphy and A. Hodgson, J. Chem. Phys. **108**, 4199 (1998).
[20] E. Watts and G. O. Sitz, J. Chem. Phys. **111**, 9791 (1999).
[21] E. Watts, G. O. Sitz, D. A. McCormack, G.-J. Kroes, R. A. Olsen, J. A. Groeneveld, J. N. P. van Stralen, E. J. Baerends, and R. C. Mowrey, J. Chem. Phys. **114**, 495 (2001).
[22] A. Groß, Surf. Sci. **500**, 347 (2002).
[23] J. L. Gland, B. A. Sexton, and G. B. Fisher, Surf. Sci. **95**, 587 (1980).
[24] H. Steininger, S. Lehwald, and H. Ibach, Surf. Sci. **123**, 1 (1982).
[25] A. C. Luntz, J. Grimblot, and D. E. Fowler, Phys. Rev. B **39**, 12903 (1989).
[26] W. Wurth, J. Stöhr, P. Feulner, X. Pan, K. R. Bauchspiess, Y. Baba, E. Hudel, G. Rocker, and D. Menzel, Phys. Rev. Lett. **65**, 2426 (1990).
[27] C. Puglia, A. Nilsson, B. Hernnäs, O. Karis, P. Bennich, and N. Mårtensson, Surf. Sci. **342**, 119 (1995).
[28] J. Wintterlin, R. Schuster, and G. Ertl, Phys. Rev. Lett. **77**, 123 (1996).
[29] K. Gustafsson and S. Andersson, J. Chem. Phys. **120**, 7750 (2004).
[30] A. Groß, in *The Chemical Physics of Solid Surfaces*, edited by D. P. Woodruff (Elsevier, Amsterdam, 2003), Vol. 11, Chap. 1.
[31] C. T. Campbell, G. Ertl, H. Kuipers, and J. Segner, Surf. Sci. **107**, 220 (1981).
[32] A. C. Luntz, M. D. Williams, and D. S. Bethune, J. Chem. Phys. **89**, 4381 (1988).
[33] C. T. Rettner and C. B. Mullins, J. Chem. Phys. **94**, 1626 (1991).
[34] A. E. Wiskerke, F. H. Geuzebroek, A. W. Kleyn, and B. E. Hayden, Surf. Sci. **272**, 256 (1992).
[35] B. C. Stipe, M. A. Rezaei, W. Ho, S. Gao, M. Persson, and B. I. Lundqvist, Phys. Rev. Lett. **78**, 4410 (1997).
[36] P. D. Nolan, B. R. Lutz, P. L. Tanaka, J. E. Davis, and C. B. Mullins, Phys. Rev. Lett. **81**, 3179 (1998).
[37] P. D. Nolan, B. R. Lutz, P. L. Tanaka, J. E. Davis, and C. B. Mullins, J. Chem. Phys. **111**, 3696 (1999).
[38] A. Eichler and J. Hafner, Phys. Rev. Lett. **79**, 4481 (1997).
[39] A. Eichler, F. Mittendorfer, and J. Hafner, Phys. Rev. B **62**, 4744 (2000).
[40] J. P. Perdew, J. A. Chevary, S. H. Vosko, K. A. Jackson, M. R. Pederson, D. J. Singh, and C. Fiolhais, Phys. Rev. B **46**, 6671 (1992).
[41] A. Groß, A. Eichler, J. Hafner, M. J. Mehl, and D. A. Papaconstantopoulos, Surf. Sci. **539**, L542 (2003).
[42] G. Kresse and J. Furthmüller, Phys. Rev. B **54**, 11169 (1996).
[43] G. Kresse and J. Furthmüller, Comput. Mater. Sci. **6**, 15 (1996).
[44] M. J. Mehl and D. A. Papaconstantopoulos, Phys. Rev. B **54**, 4519 (1996).
[45] A. Groß, M. Scheffler, M. J. Mehl, and D. A. Papaconstantopoulos, Phys. Rev. Lett. **82**, 1209 (1999).
[46] D. A. Papaconstantopoulos and M. J. Mehl, J. Phys.: Condens. Matter **15**, R413 (2003).
[47] C. M. Goringe, D. R. Bowler, and E. Hernández, Rep. Prog. Phys. **60**, 1447 (1997).
[48] F. Kirchhoff, M. J. Mehl, N. I. Papanicolaou, D. A. Papaconstantopoulos, and F. S. Khan, Phys. Rev. B **63**, 195101 (2001).
[49] A. Groß and M. Scheffler, J. Vac. Sci. Technol. A **15**, 1624 (1997).
[50] A. Groß and M. Scheffler, Phys. Rev. B **57**, 2493 (1998).
[51] H. F. Busnengo, W. Dong, and A. Salin, Chem. Phys. Lett. **320**, 328 (2000).
[52] C. Crespos, H. F. Busnengo, W. Dong, and A. Salin, J. Chem. Phys. **114**, 10954 (2001).
[53] M. Beutl, K. D. Rendulic, and G. R. Castro, Surf. Sci. **385**, 97 (1997).
[54] P. Gambardella, Ž. Šljivančanin, B. Hammer, M. Blanc, K. Kuhnke, and K. Kern, Phys. Rev. Lett. **87**, 056103 (2001).
[55] G. R. Darling and S. Holloway, Surf. Sci. **304**, L461 (1994).
[56] A. Groß, J. Chem. Phys. **102**, 5045 (1995).
[57] A. Groß and M. Scheffler, Chem. Phys. Lett. **263**, 567 (1996).
[58] J. E. Hurst, L. Wharton, K. C. Janda, and D. J. Auerbach, J. Chem. Phys. **78**, 1559 (1983).